Eur. Phys. J. B **49**, 25–35 (2006)
DOI: 10.1140/epjb/e2006-00024-2

THE EUROPEAN PHYSICAL JOURNAL B

Asymmetric quantum dots in an applied electric field: discontinuous electron density

S. Pleutin[a]

Physikalisches Institut, Albert-Ludwigs-Universität, Hermann-Herder-Straße 3, 79104 Freiburg, Germany

Received 30 July 2005 / Received in final form 30 November 2005
Published online 31 January 2006 –

Abstract. We consider non-interacting electrons in asymmetric quantum dots with either hard wall boundary conditions (rectangular quantum dots) or anharmonic confinement (elliptic quantum dots). In both cases, due to finite size effects, a homogeneous electric field applied along the long axis is shown to induce abrupt changes in the electron density, parallel and perpendicular to the field direction. Making use of this property, we propose a pure electrical mechanism to control the magnitude of the effective exchange interaction between two weakly-coupled quantum dots. This kind of system has been proposed recently as possible realization of quantum gates for quantum computation.

PACS. 73.22.-f Electronic structure of nanoscale materials: clusters, nanoparticles, nanotubes, and nanocrystals – 85.35.Be Quantum well devices (quantum dots, quantum wires, etc.)

1 Introduction

Due to remarkable advances in microfabrication techniques, it is possible nowadays to study the spectroscopic properties of single systems at mesoscopic or even nanoscopic scale. These can be semiconductor quantum dots [1,2], ultrasmall metallic particles [3] or, organic molecules [4], for instance. This opens many new perspectives for fundamental physics but also for the development of new technologies. Indeed, on the one hand, it is possible to study properties of very small systems where quantum phenomena are prominent; on the other hand, one may think of applying these new properties to go one step further on the way to extreme miniaturization towards electronics at the nanometer scale. In this context, to understand the behavior of small systems under the influence of external excitations is a central issue, with the aim to control the parameters of future nanodevices by external sources. Here we focus our attention on DC homogeneous electric fields applied on semiconductor quantum dots. Since in all the above mentioned systems the electrons are confined in a very small region of space giving rise to discrete electronic spectra, we expect they should share common features despite important differences. Therefore, we believe some of the conclusions obtained below are relevant for metallic particles and large organic molecules, as well.

The problem of the influence of a DC electric field on electronic systems has attracted a lot of interest since many years. In any case, we don't want to review this tremendous amount of articles but, instead, we content ourselves to cite those of direct use for us. Most often in the literature, this problem is treated in one-dimension, either for free electrons [5,6] or for electrons in a periodic potential [6,7], with the main focus on the Wannier-Stark ladder problem in the latter case. Here we investigate systems with many channels. More precisely, we don't consider Zener tunnelling between bands, but we are rather interested in effects caused by the interplay of the applied electric field that distorts the electronic levels and Pauli's principle which acts as a kind of quantum pressure.

We consider asymmetric semiconductor quantum dots, rectangular or elliptic, with characteristic sizes such that their mean level spacing ranges in the meV region. The electrons within the box are supposed to be non-interacting or, in cases with two weakly coupled dots, the Coulomb interaction is handled within the Heitler-London approximation that is more or less equivalent to first order perturbation theory. The homogeneous electric field, E, is applied parallel to the long axis. A first obvious effect of the field is to polarize the electronic cloud in the longitudinal direction i.e. parallel to the field direction. Our purpose is to investigate another effect caused by the finite size of the system. We consider two types of confinement: infinite potential wall and harmonic confinement plus a small anharmonic perturbation. In both cases, the electric field is shown to induce at a critical value, E_c, abrupt changes in the electron density parallel and perpendicular to the field direction. Despite the fact that no interband coupling exists, the electric field modifies the electron distribution among the different bands. The net

[a] e-mail: pleutin@physik.uni-freiburg.de

effect of this redistribution is to decrease the longitudinal polarization and to push the electrons toward the surfaces of the well perpendicularly to the field. This effect is discussed here on the basis of simple models, with the purpose of pointing out the basic mechanism at its origin and its possible relevance in the context of nanophysics and quantum computation. Indeed, as a first application, we consider two lateral weakly coupled quantum dots: the electric field is shown to modify abruptly the gap between the lowest singlet and triplet states. This last point gives a way to detect experimentally the effect predicted in this work. Moreover, this property could have important applications in the context of quantum computation where similar systems were proposed as possible realization of quantum gates [8].

The paper is organized as follows. In Section 2 we investigate the case with hard wall boundary conditions, and in Section 3 the case with a harmonic confinement plus a perturbative anharmonic term. Finally, in Section 4, we present our results for two weakly coupled quantum dots.

2 Rectangular potential wells with infinite walls in an applied electric field

We start by considering a system of non-interacting electrons confined in a rectangular potential well in the xy-plane with infinite walls. The corresponding one-electron time-independent Schrödinger equation in presence of an applied electric field is

$$-\frac{\hbar^2}{2m}\nabla^2\Psi(x,y) + qEx\Psi(x,y) = \epsilon\Psi(x,y) \tag{1}$$

where m is the effective mass of the quasi-electrons, q the electron charge ($q < 0$), E the applied electric field and ϵ the energy eigenvalue. The wave functions fulfill the hard-wall boundary conditions: $\Psi(0,y) = \Psi(L_x,y) = 0$ and $\Psi(x,0) = \Psi(x,L_y) = 0$. We assume a rectangular box such that $L_x > L_y$.

Without electric field ($E = 0$), we recover one of the basic problems of quantum mechanics: the well known particle in the box problem in two dimension. The eigenenergies are given by [9]

$$\epsilon_{n_x,n_y} = \frac{\hbar^2}{2m}\left[\left(\frac{\pi n_x}{L_x}\right)^2 + \left(\frac{\pi n_y}{L_y}\right)^2\right] \tag{2}$$

where $\{n_x, n_y\} \in \mathbf{N}^* \times \mathbf{N}^*$ ($\mathbf{N}^*$ is the set of integers without 0).

With electric field ($E \neq 0$), since there is still no coupling between the x and y coordinates, the wave functions may again be written as a product: $\Psi(x,y) = \varphi(x)\xi(y)$. The corresponding energy eigenvalues are now given by $\epsilon_{n_y} = \frac{\hbar^2}{2m}\left[(\frac{\pi n_y}{L_y})^2\right] + e$, since the equation for $\xi(y)$ is the one of a particle in a one dimensional box [9]. The equation for $\varphi(x)$ reads

$$-\frac{\hbar^2}{2m}\frac{d^2}{dx^2}\varphi(x) + qEx\varphi(x) = e\varphi(x). \tag{3}$$

Solutions of this problem are well known for both infinite [5] and finite size systems [6]. We closely follow these two references.

We set $\tilde{e} = \frac{2m}{\hbar^2}e$ and $F = -\frac{2m}{\hbar^2}qE$ and write down the solution of equation (3) as a linear combination of Airy functions [10], **Ai** and **Bi**,

$$\varphi(x) = \alpha\mathbf{Ai}\left(-F^{1/3}\left[x + \frac{\tilde{e}}{F}\right]\right) + \beta\mathbf{Bi}\left(-F^{1/3}\left[x + \frac{\tilde{e}}{F}\right]\right) \tag{4}$$

where α and β are two real constants to be determined. The wave functions should vanish at the frontiers of the potential well, $\varphi(0) = \varphi(L_x) = 0$. These conditions help, on the one hand, to fix the values of α and β, and, on the other hand, to write down the secular equation that gives the set of discrete eigenvalues, $\tilde{e}$,

$$\mathbf{Ai}\big(-\tilde{e}F^{-2/3}\big)\mathbf{Bi}\big(-L_xF^{1/3} - \tilde{e}F^{-2/3}\big) - \mathbf{Ai}\big(-L_xF^{1/3} - \tilde{e}F^{-2/3}\big)\mathbf{Bi}\big(-\tilde{e}F^{-2/3}\big) = 0. \tag{5}$$

We can equivalently express the Airy functions in terms of Bessel functions of fractional order [10], $\mathbf{J}_{1/3}$ and $\mathbf{J}_{-1/3}$,

$$\mathbf{Ai}(-z) = \frac{\sqrt{z}}{3}\big(\mathbf{J}_{1/3}(\zeta) + \mathbf{J}_{-1/3}(\zeta)\big)$$
$$\mathbf{Bi}(-z) = \sqrt{\frac{z}{3}}\big(\mathbf{J}_{-1/3}(\zeta) - \mathbf{J}_{1/3}(\zeta)\big) \tag{6}$$

with $\zeta = \frac{2}{3}z^{3/2}$. The eigenvalue equation can then be rewritten as

$$\mathbf{J}_{1/3}\left(\frac{2}{3}\frac{\tilde{e}^{3/2}}{F}\right)\mathbf{J}_{-1/3}\left(\frac{2}{3}\left[L_xF^{1/3} + \tilde{e}F^{-2/3}\right]^{3/2}\right) - \mathbf{J}_{-1/3}\left(\frac{2}{3}\frac{\tilde{e}^{3/2}}{F}\right)\mathbf{J}_{1/3}\left(\frac{2}{3}\left[L_xF^{1/3} + \tilde{e}F^{-2/3}\right]^{3/2}\right) = 0. \tag{7}$$

The equations (5) and (7) can be solved numerically, but additional approximations may be applied for our purpose. Indeed, especially at weak electric field, most of the eigenvalues are such that $\tilde{e}^{3/2} \gg F$. In this case, we can make use of an asymptotic expansion of the Bessel function [10] (when $z \to +\infty$, $\mathbf{J}_\mu \sim \sqrt{2/\pi z}\cos(z - \mu\pi/2 - \pi/4)$) that greatly simplifies equation (7) to yield

$$\left[L_xF^{1/3} + \tilde{e}F^{-2/3}\right]^{3/2} - \left[\tilde{e}F^{-2/3}\right]^{3/2} = n\frac{3\pi}{2} \tag{8}$$

with $n \in \mathbf{N}^*$. The latter equation is easier to solve than equation (7) and is very reliable for large n. In fact, for all the cases we have considered, the results obtained from equation (8) are in excellent agreement with the exact ones, even for small n. To give an example, we get for $FL_x = 10^{-2}$ a relative error of 10^{-4} for the first eigenenergy, $n = 1$. The error rapidly decreases with increasing

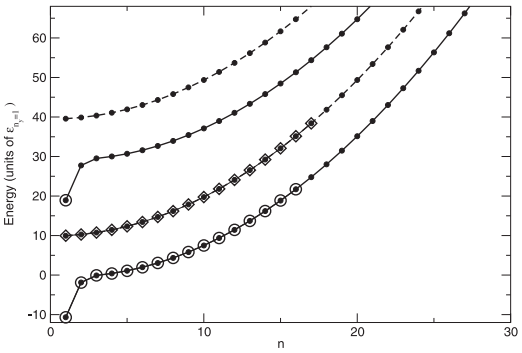

Fig. 1. The two lowest bands, $n_y = 1$ and $n_y = 2$, of a system of non-interacting electrons confined in a rectangular potential well such that $L_x = 10L_y$, in units of $\epsilon_{n_y=1} = \frac{\hbar^2}{2mL_y^2}$. The dashed curves are for $E = 0$, the full curves for $E = 0.1\frac{\hbar^2}{2m|q|L_x^3}$. The positions of the bands with electric field are shifted down by π^2, for clarity. In both cases, the dots denote the position of the discrete set of quantum states available due to finite sizes. They are labelled by the integer n, equivalent to n_x in the case without electric field. The open diamonds and the open circles are the doubly occupied levels in the case with 34 electrons and $S_z = 0$, without and with electric field, respectively. The electric field induces a change in the set of occupation numbers, the ground state changing from 1^{34} to $1^{32}2^2$ (see text): two electrons jump from the band $n_y = 1$ to the band $n_y = 2$.

values of n. Starting from equation (8), we may further assume that $\tilde{e} \gg FL_x$. We can then expand the first term of equation (8) in powers of $\frac{FL_x}{\tilde{e}}$. At first order one gets, as expected, the non-interacting electron spectrum $\tilde{e} \simeq (\frac{n\pi}{L_x})^2$. Details about the opposite limit where $\tilde{e} \ll FL_x$ can be found in reference [6]. In any case, the spectrum of the system with electric field is given by

$$\epsilon_{n_y}(\mathcal{E}) = \frac{\hbar^2}{2m}\left[\tilde{e} + \left(\frac{\pi n_y}{L_y}\right)^2\right]. \qquad (9)$$

Examples are shown in Figure 1, for $L_x = 10L_y$. The two lowest bands, $n_y = 1$ and $n_y = 2$, are shown with and without electric field. One can notice that the distortion of the bands induced by the electric field depends on the energy or quantum number n of equation (8): it is rather strong at low energies (small n) where a change of curvature can be seen in our example, and turns into a uniform shift at higher energies (large n). At zero temperature, the ground state of the system with N_e electrons is determined by filling up successively the one-electron eigenstates according to Pauli's principle. In analogy with classifications used in atomic physics, it may be characterized by a set of occupation numbers, $A_{n_y}(E)$, that give the number of electrons in band n_y at a particular electric field. The ground state may then be characterized by the product $\prod_{n_y, A_{n_y}\neq 0} n_y^{A_{n_y}}$ meaning that the band n_y is populated by A_{n_y} electrons; it gives a representation of the ground-state electronic configuration. Since the magnitude of the perturbation is not the same for every state $\varphi(x)$, one may expect the electric field to be able to induce changes in the set of occupation numbers. Such an example is seen in Figure 1, where we have considered 34 electrons, 17 with spin up and 17 with spin down. Without electric field, only states in the lowest band are doubly occupied (this is represented by the open diamonds in Fig. 1) and in such a way that the lowest unoccupied level is in the second band. With an electric field, the perturbation of the lowest level of the second band is larger than the perturbation of the highest occupied level of the first band. Consequently, an abrupt change in the set of occupation number occurs once the electric field becomes larger than a critical field, E_c, for which the lowest occupied and the highest unoccupied levels become degenerate. The value of this critical field dramatically depends on the geometry of the box: we obtain for instance, $E_c \simeq 0.1\frac{\hbar^2}{2m|q|L_x^3}$ for $L_x = 10L_y$ and $E_c \simeq 0.01\frac{\hbar^2}{2m|q|L_x^3}$ for $L_x = 9.8L_y$. For the case shown in Figure 1, the ground state is characterized by the products 1^{34}, for $E < E_c$, and $1^{32}2^2$, for $E \geq E_c$.

Since a particular band, characterized by n_y, is associated with a particular function $\xi_{n_y}(y) = \sqrt{\frac{2}{L_y}}\sin(\frac{\pi n_y}{L_y}y)$, to a change in the occupation numbers, A_{n_y}, corresponds a change in the electron density in the direction perpendicular to the applied electric field. This is well observed in the transverse electron density, $\rho^T(y, E)$, which is the density with the x variable integrated out

$$\rho^T(y,E) = \int_0^{L_x} dx\rho(x,y,E) = \frac{4}{N_e L_y}\sum_{n_y} A_{n_y}(E)\sin^2\frac{\pi n_y}{L_y}y \qquad (10)$$

where the superscript T is for *Transverse*. This quantity is expressed by the sum of the occupation numbers, A_{n_y}, weighted by the square of the corresponding transverse wavefunction, ξ_{n_y}. An example is shown in Figure 2, where we have plotted the change of transverse density defined as the difference of $\rho^T(y, E)$ with and without electric field

$$\delta\rho^T(y,E) = \rho^T(y,E) - \rho^T(y,0) = \frac{4}{N_e L_y}\sum_{n_y}\left[A_{n_y}(E) - A_{n_y}(0)\right]\sin^2\frac{\pi n_y}{L_y}y. \qquad (11)$$

Since $A_{n_y}(E) = A_{n_y}(0)$ for $E < E_c$, this is a discontinuous function of the electric field, non-vanishing for $E > E_c$ only. In our example ($L_x = 10L_y$, $N_e = 34$), at $E = E_c = 0.1\frac{\hbar^2}{2m|q|L_x^3}$ two electrons jump from the band $n_y = 1$ to the band $n_y = 2$ inducing the changes seen in Figure 2: electrons leave the center of the dot to reach the two edges parallel to the applied electric field. Of course, this jump produces also a decrease of the longitudinal electric-polarization i.e. in the x-direction, an example is given in the next section.

Before closing this section, we would like to comment a little on the neglect of Coulomb interaction. In particular, the screening of the applied electric field by the electrons

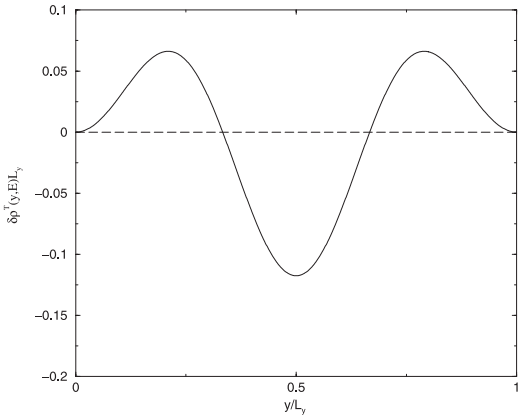

Fig. 2. Changes in the transverse electron density, $\delta\rho^T(y,E)$, of a system of non-interacting electrons confined in a rectangular box with hard-wall boundary conditions for $E < E_c$ (dashed curve) and for $E > E_c$ (full curve). At a critical value, E_c, an electric field induces abrupt changes in the set of occupation numbers, A_{n_y}, defining the ground state (see text) and, consequently, in the transverse electron density. In this example, the ground state changes from 1^{34} to $1^{32}2^2$. The value of the critical field depends on the geometry of the well: it is $E_c \simeq 0.1\frac{\hbar^2}{2m|q|L_x^3}$ for $L_x = 10L_y$ and $E_c \simeq 0.01\frac{\hbar^2}{2m|q|L_x^3}$ for $L_x = 9.8L_y$, for instance.

is not taken into account in this work but we expect this effect would not change qualitatively our conclusions. Indeed, it was shown recently, in the context of molecular electronics, that the screening properties of strictly one dimensional systems or molecular wires are rather inefficient [11]: to consider the electric field to be unscreened is then a good approximation in this case that should remain valid for the quasi-one dimensional systems that we investigate, where only few channels are occupied.

3 Anharmonic oscillators with an applied electric field

As a next example, we consider electrons within a two dimensional box as in the previous section, but with a more realistic harmonic confinement. We assume the potential to be asymmetric (elliptic dot) and we add a weak anharmonic term in the direction of the applied electric field. We could also add anharmonicity in the y-direction but this is not essential in the present context. The corresponding one-particle time-independent Schrödinger equation is

$$-\frac{\hbar^2}{2m}\nabla^2\Psi(x,y) + \left[\frac{1}{2}m\omega_x^2x^2 + \frac{1}{2}m\omega_y^2y^2 + \lambda x^4 + qEx\right] \times \Psi(x,y) = \epsilon\Psi(x,y) \quad (12)$$

where we assume $\omega_x < \omega_y$ and $\lambda > 0$. In practice, there is always anharmonic contributions in the electronic spectrum. Such contributions were for instance invoked to account for the depression of the ground state energy observed in tunnelling spectroscopy [12,13]. It was moreover demonstrated recently that a single quantum dot behaves as an anharmonic emitter from photoluminescence spectroscopy where photon antibunching were observed [14]. Such anharmonicities can be due to confinement irregularities, for instance. More fundamentally, the potential should be determined self-consistently starting from a more microscopic description of the dot that includes Coulomb interaction. Following this way, to get the precise shape of the confining potential is however a difficult task that was shown to depend on several parameters and properties such as the temperature, the doping level, the Fermi level pinning properties of lateral surfaces and the lateral dimensions [15]. It is the result of complex electrostatic screening processes that give nevertheless evident signs of anharmonicity for relevant choices of the parameters [15]. In any case, the anharmonic term introduces a field-dependent perturbation which does not exist in the pure harmonic case and which is crucial for our purpose, as will be explained in the following two subsections.

3.1 Harmonic oscillators in an electric field

First, we neglect the anharmonic term and consider the case without electric field, $\lambda = E = 0$. In this case one recovers the very well known two dimensional harmonic oscillator problem. The wave-functions are written as products, $\Psi_{n_x,n_y}(x,y) = \varphi_{n_x}(x)\varphi_{n_y}(y)$, with

$$\varphi_{n_u}(u) = \left(\frac{\beta_u^2}{\pi}\right)^{1/4} \frac{1}{\sqrt{2^{n_u}n_u!}} e^{-\beta_u^2u^2/2} H_{n_u}(\beta_u u) \quad (13)$$

where $u = x/y$, $\beta_u = \sqrt{\frac{m\omega_u}{\hbar}}$ and H_{n_u} is Hermite's polynomial of order n_u. The corresponding eigenenergies are

$$\epsilon_{n_x,n_y} = \left(n_x + \frac{1}{2}\right)\hbar\omega_x + \left(n_y + \frac{1}{2}\right)\hbar\omega_y \quad (14)$$

where n_x and n_y are two integers [9].

With an applied electric field but without anharmonicity, $\lambda = 0$ and $E \neq 0$, the overall spectrum of the harmonic oscillator is shifted by $-\frac{q^2E^2}{2m\omega_x^2}$ which corresponds to a shift of the center of mass by $-\frac{qE}{m\omega_x^2}$, in the x-direction. The eigenfunctions become [9]

$$\varphi_{n_x}(x,E) = \left(\frac{\beta_x^2}{\pi}\right)^{1/4} \frac{1}{\sqrt{2^{n_x}n_x!}} e^{-\beta_x^2\left(x+\frac{qE}{m\omega_x^2}\right)^2/2} \times H_{n_x}\left(\beta_x\left(x + \frac{qE}{m\omega_x^2}\right)\right). \quad (15)$$

Since the perturbation induced by the field is the same for all eigenenergies, there is no change in the set of occupation numbers, A_{n_y}, and, thereby, in the electron density. This property is very peculiar to the harmonic confinement. The situation is very different with anharmonicity as it is shown in the next subsection.

3.2 Effects of anharmonicity

The anharmonic contribution breaks the well known property of the harmonic oscillator with electric field discussed above: with $\lambda \neq 0$, the eigenenergies are not all shifted by the same quantity but, instead, the changes induced by the field depend on the quantum number n_x as for the case treated in Section 2. This is true whatever the magnitude of λ. This is shown here by considering λ very small compared to the other energy scales, $\lambda/\beta_x^4 \ll \hbar\omega_u$ $(u = x/y)$, for simplicity, but the conclusions that we obtain should be qualitatively valid out of this regime as well. It has been known that the perturbative expansion in λ is not convergent but asymptotic [16]. Yet, the perturbative results may approximate the exact one if they are restricted to low orders. We assume λ sufficiently small to consider the anharmonic term at first order in perturbation theory only. Although the range of validity of this treatment is very restricted, our purpose is mainly qualitative and aims at pointing out basic mechanisms rather than reaching a quantitative description of the phenomenon that would require more sophisticated approaches [16]. We calculate the correction

$$\begin{aligned}\Delta_{n_x}(E) &= \lambda \int_{-\infty}^{+\infty} dx \varphi_{n_x}^2(x,E) x^4 \\ &= \lambda \int_{-\infty}^{+\infty} dx \varphi_{n_x}^2(x,0) \left(x - \frac{qE}{m\omega_x^2}\right)^4. \end{aligned} \quad (16)$$

Exploiting the well known recurrence relation for Hermite's polynomials, $xH_n(x) = nH_{n-1}(x) + \frac{1}{2}H_{n+1}(x)$, and noting that the integrals with odd power of x are null, we get

$$\Delta_{n_x}(E) = \frac{3}{2}\frac{\lambda\hbar^2}{m^2\omega_x^2}\left(n_x^2 + n_x + \frac{1}{2}\right) + 6\lambda\frac{\hbar q^2 E^2}{m^3\omega_x^5}\left(n_x + \frac{1}{2}\right) \quad (17)$$

plus an overall shift of the spectrum, $\lambda\frac{q^4E^4}{m^4\omega_x^8}$, that plays no role here; thus we neglect it in the following. The last term of equation (17) is driven by anharmonicity and introduces the explicit dependence on the applied electric field, E, and on the quantum number, n_x, mentioned above. This type of correction also appears at higher order in perturbation theory, stressing the fact that the effects describe here occur at any λ: an applied electric field is able to change the electronic configurations of the ground state of elliptic quantum dots if anharmonicities are included. We illustrate this property below by studying one particular example.

Using equation (17) and omitting the two uniform shifts, the energies of the different levels can be determined at first order in perturbation theory: $\tilde{\epsilon}_{n_x,n_y} = \epsilon_{n_x,n_y} + \Delta_{n_x}(E)$. We consider a system with four electrons, two spin up and two spin down, so that only the two occupied and the first unoccupied levels should be considered. One should stress that in order to observe discontinuities in the electron density at reasonable electric field, the number of electrons in the dot has to be adjusted in a way to reduce the gap between the highest occupied level and the lowest unoccupied level; for our particular example, the case with 4 particles is optimal in this respect. We first introduce a parameter, δ, which control the asymmetry of the harmonic confinement: $\omega_x = \omega - \delta$ and $\omega_y = \omega + \delta$. The energies of the three lowest levels including the anharmonic corrections (17) are found to be

$$\begin{cases} \tilde{\epsilon}_{0,0}(E) = \hbar\omega + \frac{3}{4}\frac{\lambda}{\beta_x^4} + 3\lambda\frac{x_E^2}{\beta_x^2} \\ \tilde{\epsilon}_{1,0}(E) = \hbar(2\omega - \delta) + \frac{15}{4}\frac{\lambda}{\beta_x^4} + 9\lambda\frac{x_E^2}{\beta_x^2} \\ \tilde{\epsilon}_{0,1}(E) = \hbar(2\omega + \delta) + \frac{3}{4}\frac{\lambda}{\beta_x^4} + 3\lambda\frac{x_E^2}{\beta_x^2} \end{cases} \quad (18)$$

where we have introduced $x_E = -\frac{qE}{m\omega_x^2}$, the shift of the center of mass induced by the electric field [9]. At a critical field, E_c, the ground state electronic configuration, $\prod_{n_y} n_y^{A_{n_y}}$, changes from 0^4 to $0^2 1^2$. The critical field is such that $\tilde{\epsilon}_{1,0}(E_c) = \tilde{\epsilon}_{0,1}(E_c)$; within our approximation it is given by

$$E_c = \frac{\hbar\omega_x\beta_x}{|q|}\sqrt{\frac{2\hbar\delta\beta_x^4 - 3\lambda}{6\lambda}}. \quad (19)$$

This change abruptly modifies the electron density in both direction, x and y, which can be calculated, at our level of approximation, by using the wave functions (13) and (15).

As already discussed for the case of hard-wall boundary confinement, for $E \geq E_c$ the electronic cloud suddenly swells in the y-direction, perpendicularly to the applied field. The change of density in the transverse direction is given by

$$\delta\rho^T(y,E) = \frac{1}{2}\sqrt{\frac{\beta_y^2}{\pi}} e^{-\beta_y^2 y^2}\left(2\beta_y^2 y^2 - 1\right)\Theta(E - E_c) \quad (20)$$

where $\Theta(x)$ is the usual step function

$$\Theta(x) = \left\{ \begin{array}{lll} 0, & \text{if} & x < 0 \\ 1, & \text{if} & x \geq 0 \end{array} \right\}. \quad (21)$$

Results for our example are shown in Figure 3: electrons are transferred from the center to the edges of the elliptic dot parallel to the direction of the field.

The center of mass of the electronic system is continuously shifted by x_E in the longitudinal direction (the x-direction) when the electric field is tuned. In addition, at the transition, $E = E_c$, the internal structure of the electronic cloud is modified in this direction too. To characterize the changes, we may consider the difference between the longitudinal electron density i.e. the electron density where the y-coordinate has been integrated out, taken at two different values of the field, E_c^+ and E_c^-, slightly above and below the transition, E_c, respectively:

$$\begin{aligned}\delta\rho^L(x, E_c^+, E_c^-) &= \rho^L(x, E_c^+) - \rho^L(x, E_c^-) \\ &= \frac{1}{2}\sqrt{\frac{\beta_x^2}{\pi}} e^{-\beta_x^2(x - x_E)^2}\left(1 - 2\beta_x^2(x - x_E)^2\right) \end{aligned} \quad (22)$$

where $\rho^L(x) = \int_{-\infty}^{+\infty} dy \rho(x,y)$, ρ the electron density. Results for our example are shown in Figure 4 where we have

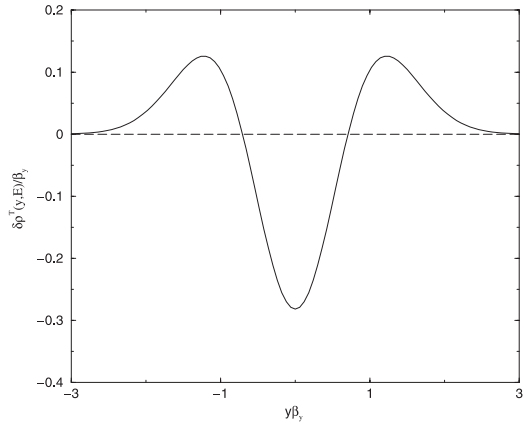

Fig. 3. Changes in the transverse electron density, $\delta\rho^T(y,E)$, of non-interacting electrons trapped in a harmonic potential with an additional weak anharmonic term, λx^4, for $E < E_c$ (dashed curve) and for $E > E_c$ (full curve). In our example, the ground state configuration, $\prod n_y^{A_{n_y}}$, changes from 0^4 to $0^2 1^2$, at $E = E_c$. As a consequence of that, some electrons leave the center of the dot towards the edges parallel to the direction of the applied field.

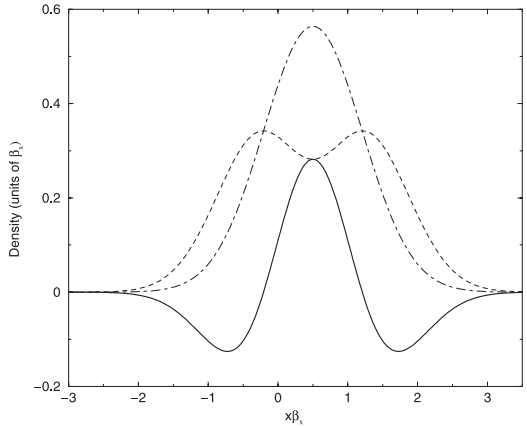

Fig. 4. Changes of electron density at $E = E_c$, in the longitudinal direction (parallel to the applied field) of non-interacting electrons trapped in a harmonic potential with an additional weak anharmonic term, λx^4. In our example, the ground state configuration, $\prod n_y^{A_{n_y}}$, changes from 0^4 to $0^2 1^2$, at $E = E_c$. The dashed lines show the longitudinal density at a value of the field slightly smaller than E_c. The dotted-dashed lines show the longitudinal density at a value of the field slightly higher than E_c. The full lines show the changes in the longitudinal density at the transition: electrons are transferred from the edges to the center of the dot. Here, we take $\beta_x x_E = 0.5$ (see text).

taken $\beta_x x_E = 0.5$: electrons are transferred from the edges perpendicular to the direction of the field to the center of the dot.

In conclusion, at the transition the electronic cloud grows in the transverse direction (y-direction) but is slightly contracted in the longitudinal direction (x-direction). For quantum dots in GaAs, $\hbar\omega_x$ is about a few meV that corresponds to an effective length $1/\beta_x$ of a few tens of nanometers; with these conditions a typical value for the critical field, at which the transition should occur, can be estimated with equation (19) to be $E_c \approx 10^{-5}$ Vm^{-1}, a value commonly used in most experimental situations.

4 Two laterally coupled quantum dots

The effect pointed out above should have consequences in various experimental situations. In this last section we propose an experimental set-up that should enable to detect it. It is inspired by a proposal made in the late 90's to use semiconductor quantum dots as building blocks for possible future quantum computers [8,17,18]. Following reference [17], we consider two lateral quantum dots weakly tunnel-coupled [1] (see Fig. 5), described by the following model

$$\hat{H} = \sum_\alpha \left(-\frac{\hbar^2}{2m}\nabla_\alpha^2 + V(x_\alpha, y_\alpha) + \lambda x_\alpha^4 + qEx_\alpha \right) + \frac{1}{2}\sum_{\alpha\neq\beta} \frac{q^2}{\kappa|\mathbf{r}_\alpha - \mathbf{r}_\beta|} \quad (23)$$

with

$$V(x_\alpha, y_\alpha) = \frac{1}{2}m\omega_x^2 x_\alpha^2 + \frac{1}{2}m\omega_y^2 \frac{(y_\alpha^2 - a^2)^2}{4a^2} \quad (24)$$

where the summation is over the particle indices, α and β. The first term in brackets in equation (23) describes non-interacting electrons in the xy-plane in a confined potential. The coupling between the two quantum dots is modeled by the quartic potential $V(x,y)$: it includes tunnelling of electrons and is well approximated by two separate harmonic potentials when the distance $2a$ between the dots is large compared to the effective length $1/\beta_y$. Compared to reference [17] we add the anharmonic contribution and an applied electric field perpendicular to the line joining the centers of the two quantum dots. The second term of equation (23) is the Coulomb interaction; κ is the dielectric constant and $\mathbf{r}_\alpha$ is the vector coordinates of the electron α, in the 3D space.

By grouping the terms differently we can rewrite the Hamiltonian $\hat{H}$ as follows

$$\hat{H} = \sum_{i=1,2} \hat{h}_i(\mathbf{r}_\alpha) + \hat{W}\mathbf{r}_\alpha) + \hat{C}(\mathbf{r}_\alpha, \mathbf{r}_\beta) \quad (25)$$

where

$$\hat{h}_{1/2}(\mathbf{r}_\alpha) = \sum_\alpha \left(-\frac{\hbar^2}{2m}\nabla_\alpha^2 + \frac{1}{2}m\omega_x^2 x_\alpha^2 + \frac{1}{2}m\omega_y^2 (y_\alpha \pm a)^2 + \lambda x_\alpha^4 + qEx_\alpha \right) \quad (26)$$

is the Hamiltonian for the isolated dot 1 (2) centered at $y = -a$ ($y = +a$) (see Fig. 5),

$$\hat{W}(\mathbf{r}_\alpha) = \sum_\alpha \frac{1}{2}m\omega_y^2 \left(\frac{(y_\alpha^2 - a^2)^2}{4a^2} - (y_\alpha + a)^2 - (y_\alpha - a)^2 \right) \quad (27)$$

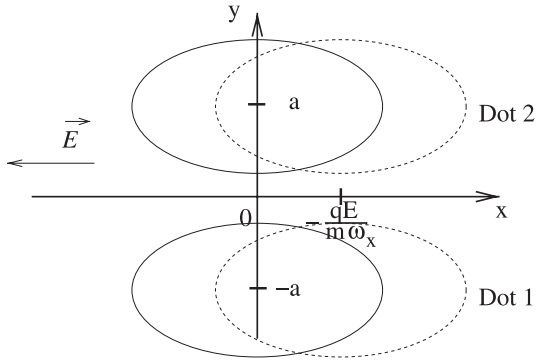

Fig. 5. Two laterally coupled elliptic quantum dots with a harmonic confinement such that $\omega_x < \omega_y$ (full lines). An applied electric field along the x-axis shifts the position of the center of mass of the two quantum dots, supposed to be identical, by $x_E = -\frac{qE}{m\omega_x}$ (dashed lines).

is the potential obtained by subtracting to V the harmonic contributions added to get equation (26) and $\hat{C}(\mathbf{r}_\alpha, \mathbf{r}_\beta) = \frac{1}{2}\sum_{\alpha\neq\beta} \frac{q^2}{\kappa|\mathbf{r}_\alpha - \mathbf{r}_\beta|}$ is the Coulomb interaction. In the following we use equation (25) to perform our calculations.

We assume the two dots to be weakly coupled, meaning that either the distance between them or the interdot barrier is large. With our specific choice of confinement potential [17], equation (24), these two quantities are intimately related i.e. it is equivalent to increase or decrease the interdot distance and the interdot barrier. In the following, we assume $a > 1/\beta_y$. In this case, the overlap between two wavefunctions centered on different dots is small and the tunnelling probability of an electron from one dot to the other is weak: the two dots can then be considered, at first approximation, as being uncoupled and the analysis that we have done in the previous section for one single dot is relevant for the coupled system. We consider the case with a small odd number of particles in each dot, leaving one unpaired electron in dot 1 and dot 2. In this case, under our assumptions, the orbital degree of freedom may be considered to be frozen and the low-energy properties of this system dominated by the ground singlet and triplet states formed by the unpaired electrons. In these conditions, it was argued that the low energy properties should be well described by an effective Heisenberg Hamiltonian for spin 1/2 [8,17,18],

$$\hat{H}_{Heis} = J\mathbf{S_1} \cdot \mathbf{S_2} \tag{28}$$

where the spin operators $\mathbf{S_1}$ and $\mathbf{S_2}$ are associated to the spin of the unpaired electrons localized in dot 1 and dot 2, respectively. The effective exchange integral, J, can be estimated starting from the more microscopic model (23): it is defined as the energy difference between the lowest triplet and singlet states. This equivalence was already studied in details using microscopic models such as equation (23). The relevance of the Heisenberg model was demonstrated, first, for the case with two electrons using the Heitler-London and Hund-Mullinken approaches in reference [17] and a more involved molecular orbital calculation in reference [18]. Later, the multielectron case was studied in reference [19]. There, the Heisenberg model (28)

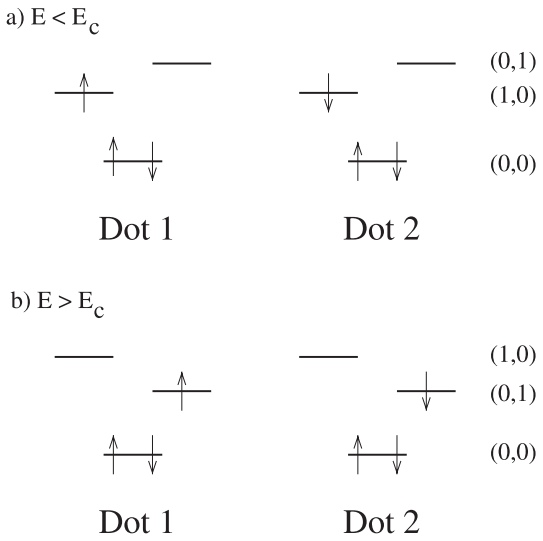

Fig. 6. Example of electronic configuration of two weakly-coupled quantum dots with three electrons in each. An applied electric field can change the energy order of the one-electron states, (n_x, n_y), in each dot. a) For $E < E_c$, the states $(0,0)$ and $(1,0)$ are populated. b) For $E > E_c$, the states $(0,0)$ and $(0,1)$ are populated. At the critical field, E_c, the unpaired electrons are transfered from the state $(1,0)$ to the state $(0,1)$ in each dot.

was shown to provide a good effective description if the degeneracies inherent of a 2D harmonic potential are lifted by an additional perturbation that breaks the circular symmetry: this is precisely the case we have considered here where the dots are asymmetric.

The magnitude of the exchange integral, J, depends on the Coulomb potential and the interdot tunnelling probability. Our basic idea may be summarized as follows. We have seen, in the previous section, that an applied electric field along the x-direction may change abruptly the electron density in the y-direction: in each dot, at a critical field, E_c, electrons are transferred from the center to the boundaries. This phenomenon should contribute to increase the overlap between the two electronic clouds centered in dot 1 and dot 2 and, therefore, it should modify the magnitude of the effective exchange integral of equation (28). Consequently, depending on the magnitude of the electric field one expects the system to be described by two different Heisenberg models, with different exchange integrals, $J^<$, for $E < E_c$, and $J^>$, for $E > E_c$. In other words, the exchange interaction of the effective spin model, equation (28), is a function of the electric field that can be written as (see Fig. 7)

$$J(E) = J^<\Theta(E_c - E) + J^>\Theta(E - E_c). \tag{29}$$

In the following, we determine these exchange integrals using a generalization of the Heitler-London method for the hydrogen molecule to a number of electrons larger than two [20]; this type of calculation is valid for large interdot distances. Within this approximation we first consider the solutions for the isolated non-interacting dots (Sect. 3) before using them to build the proper combinations of Slater

determinants to describe the whole system with interaction.

The ground state of each isolated dot has been studied in the previous section, at first order in perturbation of λ. We start by introducing new fermionic operators, $L^\dagger_{n_x,n_y,\sigma}$ ($R^\dagger_{n_x,n_y,\sigma}$) which create one electron with spin σ ($\uparrow$ or $\downarrow$) in the orbital state labelled by the quantum numbers n_x and n_y in the left (right) dot; they are associated with the wavefunctions $\varphi_{n_x}(\beta_x(x-x_E))\varphi_{n_y}(\beta_y(y+a))$ ($\varphi_{n_x}(\beta_x(x-x_E))\varphi_{n_y}(\beta_y(y-a))$ and energies $\tilde{\epsilon}_{n_x,n_y}$. We specify our study to the case with three electrons in each dot with the same number of spin up and down ($S_z=0$). In this case, it is sufficient to consider only the three lowest levels (18). Using the previous results, one concludes that the electronic configuration of the ground state changes from 0^3, for $E<E_c$, to $0^2 1^1$, for $E>E_c$ in each dot. This is depicted schematically in Figure 6. Starting from these solutions for isolated dots, we build for each of these two cases, the singlet and triplet states of the whole system. For $E<E_c$, we get

$$|\Psi^<_\pm\rangle = \frac{1}{\sqrt{2}}\left(|\Psi^<_{\uparrow\downarrow}\rangle \pm |\Psi^<_{\downarrow\uparrow}\rangle\right) \tag{30}$$

with

$$\begin{aligned}|\Psi^<_{\uparrow\downarrow}\rangle &= L^\dagger_{0,0,\downarrow}L^\dagger_{0,0,\uparrow}R^\dagger_{0,0,\downarrow}R^\dagger_{0,0,\uparrow}R^\dagger_{1,0,\downarrow}L^\dagger_{1,0,\uparrow}|0\rangle\\ |\Psi^<_{\downarrow\uparrow}\rangle &= L^\dagger_{0,0,\downarrow}L^\dagger_{0,0,\uparrow}R^\dagger_{0,0,\downarrow}R^\dagger_{0,0,\uparrow}L^\dagger_{1,0,\downarrow}R^\dagger_{1,0,\uparrow}|0\rangle\end{aligned} \tag{31}$$

and, in the same way, we get for $E>E_c$

$$|\Psi^>_\pm\rangle = \frac{1}{\sqrt{2}}\left(|\Psi^>_{\uparrow\downarrow}\rangle \pm |\Psi^>_{\downarrow\uparrow}\rangle\right) \tag{32}$$

with

$$\begin{aligned}|\Psi^>_{\uparrow\downarrow}\rangle &= L^\dagger_{0,0,\downarrow}L^\dagger_{0,0,\uparrow}R^\dagger_{0,0,\downarrow}R^\dagger_{0,0,\uparrow}R^\dagger_{0,1,\downarrow}L^\dagger_{0,1,\uparrow}|0\rangle\\ |\Psi^>_{\downarrow\uparrow}\rangle &= L^\dagger_{0,0,\downarrow}L^\dagger_{0,0,\uparrow}R^\dagger_{0,0,\downarrow}R^\dagger_{0,0,\uparrow}L^\dagger_{0,1,\downarrow}R^\dagger_{0,1,\uparrow}|0\rangle\end{aligned} \tag{33}$$

where the + sign is for the singlet, the — being for the triplet, and $|0\rangle$ is the vacuum.

Next, after evaluating the triplet and singlet energy for the two different cases,

$$\epsilon^{<,>}_\pm = \frac{\langle\Psi^{<,>}_\pm|\hat{H}|\Psi^{<,>}_\pm\rangle}{\langle\Psi^{<,>}_\pm|\Psi^{<,>}_\pm\rangle} \tag{34}$$

we can determine the exchange integrals, $J^<$ and $J^>$, of the effective Heisenberg model (28)

$$\begin{aligned}J^< &= \epsilon^<_- - \epsilon^<_+\\ J^> &= \epsilon^>_- - \epsilon^>_+\end{aligned} \tag{35}$$

given by the difference between the triplet and the singlet energy [17].

The wavefunctions used to describe the system are not all orthogonal since

$$S_{n_y,n'_y} = \int_{-\infty}^{+\infty}\varphi_{n_y}(y+a)\varphi_{n'_y}(y-a) \neq 0. \tag{36}$$

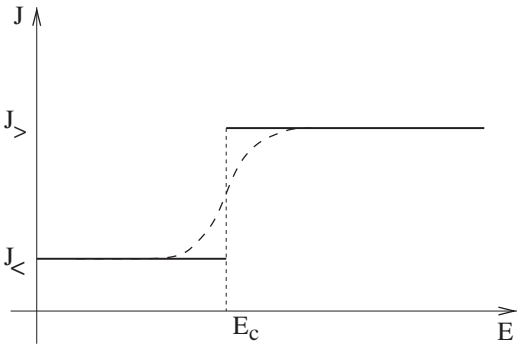

Fig. 7. Exchange integral of the effective Heisenberg model (28), describing the low-electronic properties of two weakly coupled quantum dots with one unpaired electron in each, as function of the applied electric field. At a critical field, E_c, the electronic structure of each dot is modified which causes a sudden jump of J, changing from $J^<$ to $J^>$. At first approximation the jump appears as a discontinuity (full curve); in a more refined version, it is continuous (dashed curve). This property may be used (i) to detect the effect predicted in this work and, (ii) to perform a *swap* operation (see text) in the context of quantum computation.

This property makes the calculation of the energies (34) more cumbersome. However, using the wavefunction (13), we can estimate that the overlap behaves as $S_{n_y,n'_y} =$ (Polynomial of a) $\times\, e^{-\beta_y^2 a^2}$. Since we assume a to be relatively large with respect to $1/\beta_y$, a reasonably good approximation consists to keep in the calculation, terms of the type $S^m_{n_y,n'_y}$ with $m\leq 2$. With this simplification, after lengthy but straightforward calculations, we obtain

$$\begin{aligned}J^< = e^{-2\beta_y^2a^2}\Bigg[&\frac{q^2}{\kappa}R^<_K\mathbf{K}\left(\frac{\sqrt{\beta_y^2-\beta_x^2}}{\beta_y}\right)\\ &+\frac{q^2}{\kappa}R^<_E\mathbf{E}\left(\frac{\sqrt{\beta_y^2-\beta_x^2}}{\beta_y}\right)+\frac{3}{2}\hbar\omega_y\left(1-3\beta_y^2a^2\right)\Bigg]\end{aligned} \tag{37}$$

with

$$\begin{cases}R^<_K = \sqrt{\frac{2}{\pi}}\beta_x\dfrac{12\beta_x^4+\beta_y^4-15\beta_x^2\beta_y^2}{2(\beta_y^2-\beta_x^2)^2}\\ R^<_E = \sqrt{\frac{2}{\pi}}\beta_x\dfrac{6\beta_y^4-5\beta_x^2\beta_y^2}{(\beta_y^2-\beta_x^2)^2}\end{cases} \tag{38}$$

and

$$\begin{aligned}J^> = e^{-2\beta_y^2a^2}\Bigg[&\frac{q^2}{\kappa}R^>_K\mathbf{K}\left(\frac{\sqrt{\beta_y^2-\beta_x^2}}{\beta_y}\right)+\frac{q^2}{\kappa}R^>_E\mathbf{E}\\ &\times\left(\frac{\sqrt{\beta_y^2-\beta_x^2}}{\beta_y}\right)+\hbar\omega_y\left(2\beta_y^2a^2-1\right)\left(-\frac{3}{2}+\frac{7}{2}\beta_y^2a^2-9\beta_y^4a^4\right)\Bigg]\end{aligned} \tag{39}$$

with

$$\begin{cases} R_K^> = \sqrt{\frac{2}{\pi}}\beta_x \frac{-\beta_x^4+(48\beta_y^4a^4-48\beta_y^2a^2+15)\beta_y^4+(8\beta_y^2a^2+2)\beta_x^2\beta_y^2}{2\beta_y^2(\beta_y^2-\beta_x^2)} \\ R_E^> = \sqrt{\frac{2}{\pi}}\beta_x \frac{\beta_x^2+(24\beta_y^4a^4-20\beta_y^2a^2+5)\beta_y^2}{\beta_y^2-\beta_x^2} \end{cases} \tag{40}$$

where **K** and **E** are the complete elliptic integrals of the first and second kind, respectively, defined as [10]

$$\mathbf{K}(k) = \int_0^{\pi/2} \frac{d\theta}{\sqrt{1-k^2\sin^2\theta}},$$
$$\mathbf{E}(k) = \int_0^{\pi/2} d\theta\sqrt{1-k^2\sin^2\theta}. \tag{41}$$

Some details about the calculation of the equations (37) and (39) are summarized in the appendix below.

Although, the two expressions (37) and (39) are only valid in the regime of weak anharmonicity, $\lambda/\beta_x^4 \ll \hbar\omega_{x/y}$, and large interdot distances, $\beta_y a > 1$, they allow us to illustrate our purpose. Indeed, they show that the exchange integral can be significantly modified by applying an electric field perpendicular to the axis joining the two dots. Taking relevant numerical values for dots in GaAs [17], $\hbar\omega_y = 3$ meV, which corresponds to $1/\beta_y = 20$ nm, and $\beta_y q^2/\kappa/\hbar\omega_y = 2.1$ and specifying our system with $\beta_y a = 1.3$, we get for $\beta_x/\beta_y = 0.9$, $J^< = 0.15$ meV and $J^> = 0.6$ meV and, for $\beta_x/\beta_y = 0.95$, $J^< = 0.19$ meV and $J^> = 3.13$ meV. We estimate the critical field in the latter case by using equation (19): assuming $\lambda/\beta_x^4 = 0.18$ meV, we obtain $E_c = 35 \times 10^{-7}$ Vm^{-1}. In both cases, the energy difference between the singlet and triplet states is large enough to be probed experimentally, as it was done in reference [21] for two coupled dots with an exchange energy tuned by an applied magnetic field as suggested in reference [17]. However, one should keep in mind that the numerical values given above have to be considered with much care since our approximation to treat the anharmonic term is very restricted. Our work is mostly qualitative and the numerical applications serve to give orders of magnitude only.

Up to now we have considered the states $|\Psi_\pm^<\rangle$ and $|\Psi_\pm^>\rangle$ as being orthogonal. In reality, couplings exist between the states $|\Psi_+^<\rangle$ and $|\Psi_-^<\rangle$, on the one hand, and the states $|\Psi_+^>\rangle$ and $|\Psi_-^>\rangle$, on the other hand,

$$\langle\Psi_\pm^<|\hat{H}|\Psi_\pm^>\rangle = I_\pm \neq 0 \tag{42}$$

due to Coulomb interaction. These terms , $I_\pm$, mix the corresponding states together and the following linear combinations have to be considered

$$\begin{cases} |\Psi_+\rangle = \alpha_+|\Psi_+^<\rangle + \beta_+|\Psi_+^>\rangle \\ |\Psi_-\rangle = \alpha_-|\Psi_-^<\rangle + \beta_-|\Psi_-^>\rangle \end{cases} \tag{43}$$

where the value of the coefficients $\alpha_\pm$ and $\beta_\pm$ depends on the applied electric field: at the transition, $E = E_c$, $|\alpha_\pm| = |\beta_\pm| = 1/2$ to become for electric field sufficiently away from E_c, $|\alpha_\pm| \simeq 1$ and $|\beta_\pm| \simeq 0$ for $E < E_c$ and $|\alpha_\pm| \simeq 0$ and $|\beta_\pm| \simeq 1$ for $E > E_c$. Consequently, in place of the discontinuous function presented above, equation (29), we get a continuous function changing from $J^<$ to $J^>$ as shown schematically in Figure 7. The width of the transition region is controlled by the magnitude of the interaction, $I_\pm$. The value of J can then be monitored continuously between $J^<$ and $J^>$ by tuning the external electric field: this property may be useful in the context of quantum computation.

D. Loss and D.P. Di Vincenzo proposed to use a system of two weakly coupled quantum dots as a possible realization of quantum gate [8]. With one unpaired electron in each dot, the system is described by an effective Heisenberg model such as (28). By changing the value of the exchange energy with external sources in such a way that $\int_0^\tau dtJ(t)/\hbar = \pi$, it would be possible to perform a *swap* operation that exchanges the quantum state of dot 1 and dot 2. When combined with single-qubit operations, this operation can be used to build a quantum XOR gate that was earlier recognized to be a universal quantum gate [22]: a XOR along with single-qubit operations may be assembled to do any quantum computation. Thus, the study of quantum gates is reduced to the study of the exchange integral of the two dot system and in the way it can be controlled experimentally. Two main approaches have been proposed up to now to control $J(t)$: (i) by a local magnetic field perpendicular to the plane of the dots and; (ii) by a local electric field parallel to the axis joining the center of the two dots. Our proposal offers another possibility. With respect to the method described in reference [17], the main advantages of the mechanism proposed here are (i) to let the average charges unchanged within the two dots, quantity that would be modified by an electric field applied along the y-axis (see Fig. 5); (ii) it is easier to apply a local electric field than a local magnetic field. We should also mention that an electric field perpendicular to the coupling direction was already proposed as a possible control parameter in reference [23] but for a system of two quantum dots of different size, vertically coupled and with only one electron in each. In this case, the effect described here don't occur and the changes of J are due to the fact that the shift, x_E, induced by the electric field has different magnitude for the two dots.

In order to test if our proposal could be used to perform a *swap* operation, further additional studies should be undertaken using, on the one hand, more realistic models to describe the two dots systems and, on the other hand, including dynamics since the time evolution of J is the crucial quantity for quantum computation.

As a first remark, we would like to point out that there is no need to consider identical dots in our scenario. Both the number of particles within each dot and the geometry of the dots might be different. In such situation, the exchange integral, $J(E)$, should show two abrupt changes instead of one at two different critical field, E_{c1} and E_{c2}, characterizing the sudden electronic modifications that take place in the dot 1 and dot 2, respectively.

As a last remark, we have seen that the electric field induces degeneracy in the electronic spectrum at $E = E_c$. In this case, the Coulomb interaction should play a central role that could significantly modify our conclusions for fields close to the critical value: in particular, the total spin of the system may be changed. This kind of transitions was already studied, for instance, in reference [24], for cylinders pierced by an Aharonov-Bohm flux, and in reference [25], for single-wall carbon nanotubes with an inhomogeneous electric field.

5 Conclusion

To conclude, we summarize our main results. We have considered systems of independent-electrons trapped in a small region of space. Two confining potentials were studied as examples: hard wall boundary conditions and a harmonic potential with an additional perturbative x^4 term. In both cases, an electric field was shown to cause abrupt changes in the electron density at a critical value, E_c. These changes occur not only in the direction parallel to the field but also in the direction perpendicular to it; they can be related to finite size effects. Exploiting this outcome, we have then considered a system of two weakly coupled quantum dots and shown that an applied homogeneous electric field is able to change abruptly the difference in energy between the lowest singlet and triplet states. This property may serve to detect the effect predicted in this work and may eventually be important in the context of quantum computation, since it could be used to realize a quantum gate. Our results were obtained with the help of deliberately oversimplified models, our aim being to point out basic mechanisms. Additional studies based on more realistic descriptions of semiconductor quantum dots are needed both to confirm the relevance of the effects described in this work and to get better estimates of the values of the different parameters needed for possible experimental realization.

Appendix A: Calculation of the exchange integrals $J^<$ and $J^>$

In this appendix we give some details on the calculation of equations (37) and (39), starting from equation (34) that we rewrite as

$$\epsilon_{\pm}^{<,>} = \frac{\langle \Psi_{\pm}^{<,>} | \hat{H} | \Psi_{\pm}^{<,>} \rangle}{\langle \Psi_{\pm}^{<,>} | \Psi_{\pm}^{<,>} \rangle} = \frac{K^{<,>} \pm L^{<,>}}{S_{\pm}^{<,>}} \tag{A.1}$$

with

$$\begin{cases} K^{<,>} &= \langle \Psi_{\uparrow\downarrow}^{<,>} | \hat{H} | \Psi_{\uparrow\downarrow}^{<,>} \rangle = \langle \Psi_{\downarrow\uparrow}^{<,>} | \hat{H} | \Psi_{\downarrow\uparrow}^{<,>} \rangle \\ L^{<,>} &= \langle \Psi_{\uparrow\downarrow}^{<,>} | \hat{H} | \Psi_{\downarrow\uparrow}^{<,>} \rangle = \langle \Psi_{\downarrow\uparrow}^{<,>} | \hat{H} | \Psi_{\uparrow\downarrow}^{<,>} \rangle \\ S_{\pm}^{<,>} &= \langle \Psi_{\uparrow\downarrow}^{<,>} | \Psi_{\uparrow\downarrow}^{<,>} \rangle \pm \langle \Psi_{\uparrow\downarrow}^{<,>} | \Psi_{\downarrow\uparrow}^{<,>} \rangle. \end{cases} \tag{A.2}$$

We start by calculating the overlaps, $S_{\pm}^{<,>}$. By applying Slater's rules for matrix elements involving determinants [26] and after straightforward integrations we found

$$\begin{cases} S_{\pm}^{<} = (1 - S_{0,0}^2)^2 (1 \pm S_{0,0}^2) \\ S_{\pm}^{>} = (1 - S_{0,0})^2 (1 \pm S_{1,1}^2) + S_{0,1}^4 (1 \pm S_{0,0}^2) - 2 S_{0,1}^2 (1 \pm S_{0,0}) \end{cases} \tag{A.3}$$

where $S_{0,0} = e^{-\beta_y^2 a^2}$, $S_{0,1} = \sqrt{2} a e^{-\beta_y^2 a^2}$ and $S_{1,1} = (2\beta_y^2 - 1) e^{-\beta_y^2 a^2}$.

Assuming $\beta_y a \ll 1$, we keep in the calculation of $\epsilon_{\pm}^{<,>}$ terms up to second order in the overlap matrix element S_{n_y,n'_y} (Eq. (36)). Expending equations (A.1) and (35), we found at this level of approximation

$$\begin{cases} J^< = 2(S_{0,0}^2 K^< - L^<) \\ J^> = 2(S_{1,1}^2 K^> - L^>) \end{cases} \tag{A.4}$$

where we have moreover to keep only terms of zeroth order in S_{n_y,n'_y} in $K^{<,>}$ and terms up to second order in $L^{<,>}$. Calculating $K^{<,>}$ and $L^{<,>}$ with the help of Slater's rules [26], we get the following detailed expressions of $J^<$ and $J^>$, where we have used the Hamiltonian in the form given by equation (25) and where $\Psi_{n_x,n_y}(x,y) = \varphi_{n_x}(x)\varphi_{n_y}(y)$ (see Eq. (13)).

1. Detailed expression of $J^<$

$$\begin{aligned} J^< = 2S_{0,0}^2 \big(& 2 \int\int d\mathbf{r_1} d\mathbf{r_2} \Psi_{0,0}^2(x_1, y_1 + a) C(\mathbf{r_1}, \mathbf{r_2}) \\ & \times \Psi_{1,0}^2(x_2, y_2 + a) \\ & - \int\int d\mathbf{r_1} d\mathbf{r_2} \Psi_{0,0}(x_1, y_1 + a) \Psi_{1,0}(x_1, y_1 + a) C(\mathbf{r_1}, \mathbf{r_2}) \\ & \times \Psi_{0,0}(x_2, y_2 + a) \Psi_{1,0}(x_2, y_2 + a) \\ & + \int d\mathbf{r_1} \Psi_{1,0}^2(x_1, y_1 + a) W(\mathbf{r_1}) \\ & + 2 \int\int d\mathbf{r_1} d\mathbf{r_2} \Psi_{0,0}^2(x_1, y_1 - a) C(\mathbf{r_1}, \mathbf{r_2}) \Psi_{1,0}^2(x_2, y_2 - a) \\ & - \int\int d\mathbf{r_1} d\mathbf{r_2} \Psi_{0,0}(x_1, y_1 - a) \Psi_{1,0}(x_1, y_1 - a) C(\mathbf{r_1}, \mathbf{r_2}) \\ & \times \Psi_{0,0}(x_2, y_2 - a) \Psi_{1,0}(x_2, y_2 - a) \\ & + \int d\mathbf{r_1} \Psi_{1,0}^2(x_1, y_1 - a) W(\mathbf{r_1}) \big) \\ & - 2 \int\int d\mathbf{r_1} d\mathbf{r_2} \Psi_{1,0}(x_1, y_1 + a) \Psi_{1,0}(x_1, y_1 - a) C(\mathbf{r_1}, \mathbf{r_2}) \\ & \times \Psi_{1,0}(x_2, y_2 + a) \Psi_{1,0}(x_2, y_2 - a) \\ & - 4 S_{0,0} \int d\mathbf{r_1} \Psi_{1,0}(x_1, y_1 + a) W(\mathbf{r_1}) \Psi_{1,0}(x_1, y_1 - a). \end{aligned} \tag{A.5}$$

2. Detailed expression of $J^{>}$

$$
\begin{aligned}
J^{>} = 2S_{1,1}^2\big(2\int\int d\mathbf{r_1}d\mathbf{r_2}\Psi_{0,0}^2(x_1,y_1+a)C(\mathbf{r_1},\mathbf{r_2}) \\
\times\Psi_{0,1}^2(x_2,y_2+a) \\
-\int\int d\mathbf{r_1}d\mathbf{r_2}\Psi_{0,0}(x_1,y_1+a)\Psi_{0,1}(x_1,y_1+a)C(\mathbf{r_1},\mathbf{r_2}) \\
\times\Psi_{0,0}(x_2,y_2+a)\Psi_{0,1}(x_2,y_2+a) \\
+\int d\mathbf{r_1}\Psi_{0,1}^2(x_1,y_1+a)W(\mathbf{r_1}) \\
+2\int\int d\mathbf{r_1}d\mathbf{r_2}\Psi_{0,0}^2(x_1,y_1-a)C(\mathbf{r_1},\mathbf{r_2})\Psi_{0,1}^2(x_2,y_2-a) \\
-\int\int d\mathbf{r_1}d\mathbf{r_2}\Psi_{0,0}(x_1,y_1-a)\Psi_{0,1}(x_1,y_1-a)C(\mathbf{r_1},\mathbf{r_2}) \\
\times\Psi_{0,0}(x_2,y_2-a)\Psi_{0,1}(x_2,y_2-a) \\
+\int d\mathbf{r_1}\Psi_{0,1}^2(x_1,y_1-a)W(\mathbf{r_1})\big) \\
-2\int\int d\mathbf{r_1}d\mathbf{r_2}\Psi_{0,1}(x_1,y_1+a)\Psi_{0,1}(x_1,y_1-a)C(\mathbf{r_1},\mathbf{r_2}) \\
\times\Psi_{0,1}(x_2,y_2+a)\Psi_{0,1}(x_2,y_2-a) \\
-4S_{1,1}\int d\mathbf{r_1}\Psi_{0,1}(x_1,y_1+a)W(\mathbf{r_1})\Psi_{0,1}(x_1,y_1-a).
\end{aligned}
\tag{A.6}
$$

Starting from equations (A.5) and (A.6) and using some useful identities such as

$$
\int_0^{\pi/2} d\theta\frac{\cos^2\theta}{\sqrt{(1-k^2\sin^2\theta)^3}} = \frac{1}{k^2}\big(\mathbf{K}(k)-\mathbf{E}(k)\big)
$$

$$
\begin{aligned}
\int_0^{\pi/2} d\theta\frac{\cos^4\theta}{\sqrt{(1-k^2\sin^2\theta)^5}} = \frac{1}{3k^2}\big((k^4-k^2-2)\mathbf{K}(k) \\
-2(k^2+1)\mathbf{E}(k)\big)
\end{aligned}
\tag{A.7}
$$

we finally get the expressions (37) and (39) for $J^{<}$ and $J^{>}$, respectively.

References

1. L.P. Kouwenhoven, C.M. Marcus, P.L. McEuen, S. Tarucha, R.M. Wetervelft, N. Wingreen, in *Mesoscopic Electron Transport*, edited by L.L. Sohn, L.P. Kouwenhoven, G. Schön, NATO ASI Series **345**, (Kluwer Academic Publishers, Dordrecht, 1997)
2. S.M. Reimann, M. Manninen, Rev. Mod. Phys. **74**, 1283 (2002)
3. J. Von Delft, D.C. Ralph, Phys. Rep. **345**, 61 (2001)
4. A. Nitzan, Ann. Rev. Phys. Chem. **52**, 681 (2001)
5. L.D. Landau, E.M. Lifshitz, *Quantum Mechanics*, (Pergamon Press, Oxford, 1981)
6. A. Rabinovitch, J. Zak, Phys. Rev. B **4**, 2358 (1971)
7. G. Nenciu, Rev. Mod. Phys. **63**, 91 (1991); F. Rossi, in *Theory of Transport Properties of Semiconductor Nanostructures*, edited by E. Schöll (Chapman and Hall, London, 1998), Chap. 9
8. D. Loss, D.P. Di Vincenzo, Phys. Rev. A **57**, 120 (1998)
9. C. Cohen-Tannoudji, B. Diu, F. Laloe, *Quantum Mechanics* (Wiley-Interscience, 1987)
10. M. Abramovitz, I.A. Stegun, *Handbook of Mathematical Functions* (Dover, New York 1965)
11. S. Pleutin, H. Grabert, G.-L. Ingold, A. Nitzan, J. Chem. Phys. **118**, 3756 (2003); G.C. Liang, A.W. Ghosh, M. Paulsson, S. Datta, Phys. Rev. B **69**, 115302 (2004)
12. M. Luban, J.H. Luscombe, M.A. Reed, D.L. Pursey, Appl. Phys. Lett. **54**, 1997 (1989); M.W. Coffey, Appl. Phys. Lett. **80**, 1219 (2002)
13. M.A. Reed, J.N. Randall, R.J. Aggarwal, R.J. Matyi, T.M. Moore, A.E. Wetsel, Phys. Rev. Lett. **60**, 535 (1988)
14. P. Michler, A. Imamoğlu, M.D. Mason, P.J. Carson, G.F. Strouse, S.K. Buratto, Nature **406**, 968 (2000); P. Michler, A. Imamoğlu, A. Kiraz, C. Becher, M.D. Mason, P.J. Carson, G.F. Strouse, S.K. Buratto, W.V. Schoenfeld, P.M. Petroff, Phys. Stat. Sol. (b) **229**, 399 (2002); A. Kiraz, S. Fälth, C. Becher, B. Gayral, W.V. Schoenfeld, P.M. Petroff, L. Zhang, E. Hu, A. Imamoğlu, Phys. Rev. B **65**, 161303(R), (2002)
15. J.H. Luscombe, M. Luban, Appl. Phys. Lett. **57**, 61 (1990); J.H. Luscombe, A.M. Bouchard, M. Luban, Phys. Rev. B **46**, 10262 (1992)
16. C.M. Bender, T.T. Wu, Phys. Rev. **184**, 1231 (1969); F.T. Hioe, D. MacMillen, E. Montroll, Phys. Rep. C **43**, 305 (1978)
17. G. Burkard, D. Loss, D.P. Di Vincenzo, Phys. Rev. B **59**, 2070 (1999)
18. X. Hu, S. Das Sarma, Phys. Rev. A **61**, 062301 (2000)
19. X. Hu, S. Das Sarma, Phys. Rev. A **64**, 042312 (2001)
20. R. McWeeny, B.T. Sutcliffe, *Methods of Molecular Quantum Mechanics* (Academic Press, London, 1992)
21. S.D. Lee, S.J. Kim, J.S. Kang, Y.B. Cho, J.B. Choi, S. Park, S.-R.E. Yang, S.J. Lee, T.H. Zyung, e-print: `arXiv:cond-mat/0410044`
22. A. Barenco, D. Deutsch, A. Ekert, R. Jozsa, Phys. Rev. Lett. **74**, 4083 (1995); D.P. Di Vincenzo, Phys. Rev. A **51**, 1015 (1995)
23. G. Burkard, G. Seelig, D. Loss, Phys. Rev. B **62**, 2581 (2000)
24. S. Pleutin, Eur. Phys. J. B **43**, 405 (2005)
25. Y. Oreg, K. Byczuk, B.I. Halperin, Phys. Rev. Lett. **85**, 365 (2000)
26. J.C. Slater, Phys. Rev. **34**, 1293 (1929)